Preprint
April 2, 2013

Fluctuation dynamo driven by shear-bursts in convectively-driven magnetohydrodynamic turbulence

J. Pratt[1], A. Busse[2], and W.-C. Müller[3]

[1] Max-Planck-Institut für Plasmaphysik, 85748 Garching, Germany and Max-Planck-Institut für Sonnensystemforschung, 37191 Katlenburg-Lindau, Germany
[2] Faculty of Engineering and the Environment, University of Southampton, UK
[3] Center for Astronomy and Astrophysics, TU Berlin, Hardenbergstr. 36 10623 Berlin, Germany

April 2, 2013

ABSTRACT

Intermittent large-scale high-shear flows are found to occur frequently and spontaneously in direct numerical simulations of statistically stationary turbulent Boussinesq magnetohydrodynamic (MHD) convection. The energetic steady-state of the system is sustained by convective driving of the velocity field and small-scale dynamo action. The intermittent emergence of flow structures with strong velocity and magnetic shearing generates magnetic energy at an elevated rate over time-scales longer than the characteristic time of the large-scale convective motion. The resilience of magnetic energy amplification suggests that intermittent shear-bursts are a significant driver of dynamo action in turbulent magnetoconvection.

Key words. Turbulence – Magnetohydrodynamics (MHD) – Dynamo – Convection

X-ray observations reveal that turbulent convection agitates the outer convection layer of stars (Güdel et al. 1997; Reiners & Basri 2007; Böhm-Vitense 2008; Simon et al. 2008). Measurements also show that planetary magnetic fields can change in magnitude and orientation (McFadden & Merrill 1995; Christensen et al. 2009; Stevenson 2010; Olson et al. 2011). Dynamo action driven by turbulent convection is accepted as the origin of solar and planetary magnetic fields. Key physical processes involved in turbulent convection and implicated in the amplification of magnetic fields remain to be identified and practically understood (Zeldovich et al. 1983; Biskamp 2003). Helicity and buoyancy remain intensely interesting to the dynamo problem (Cline et al. 2003; Cattaneo et al. 2003; Weiss & Thompson 2009).

Because of the inherent nonlinearity of turbulent plasma flows, theoretical explanation of dynamo action is often approached by mean-field theory. Comparison with three-dimensional numerical simulations verifies and inspires theoretical models (Moll et al. 2011; Wilkin et al. 2007; Harder & Hansen 2005; Stanley & Glatzmaier 2010; Tobias et al. 2011). This work reports on a resilient and newly-identified feature of characteristic dynamo action in three-dimensional convectively-driven homogeneously turbulent Boussinesq magnetoconvection based on direct numerical pseudospectral simulations using the magnetohydrodynamic (MHD) fluid approximation (Chandrasekhar 1961).

Formulation of optimal boundary conditions for simulations of turbulent flows is delicate because boundaries strongly influence the structure and dynamics of the flow. The commonly-used Rayleigh Bénard boundary conditions impose a temperature gradient to drive turbulent convection by fixing the temperature on impermeable top and bottom boundaries. For the Reynolds and Rayleigh numbers achievable with current numerical capabilities, the convection-cell pattern imposed on the flow by Rayleigh Bénard boundary conditions constrains the development of buoyantly-driven turbulence.

The simulation volume considered in this work is confined by quasi-periodic rather than Rayleigh Bénard boundary conditions. The aim is to combine the conceptual simplicity of statistical homogeneity with a physically natural convective driving of the turbulent flow. The only deviation from full periodicity in our boundary conditions is the suppression of mean flows parallel to gravity; this modification suppresses the macroscopic elevator instability discussed by Calzavarini et al. (2006). In the flow allowed by these boundary conditions in our simulation we identify a robust universal process, the shear-burst, that efficiently amplifies magnetic energy at all spatial scales in convective turbulence. The simulation model we employ is idealized, but can be viewed as a volume in an astrophysical or geophysical convective turbulent flow that is small in comparison to the pressure scale height.

Our system allows the study of a turbulent fluctuation dynamo in detail since the applied boundary conditions permit shear-bursts on large spatial and temporal scales without enforcing a large-scale structuring of the turbulent flow. Hundreds of convective time-scales prove necessary for the study of the shear-bursts that arise spontaneously in simulations of steady-state convective MHD turbulence. Shear-bursts are intermittent and spatially localized around high-shear flows; they are driven primarily at multiple large length scales, which are not necessarily continuous, and vary between bursts. A single burst is not sufficient to maintain elevated magnetic energy; however, shear-bursts recur frequently, providing an elevated growth of magnetic energy over significant periods of time. We address the properties of shear-bursts and their importance for the understanding of the fluctuation-dynamo mechanism based on observations from high-resolution direct numerical simulations that span extended periods of time.

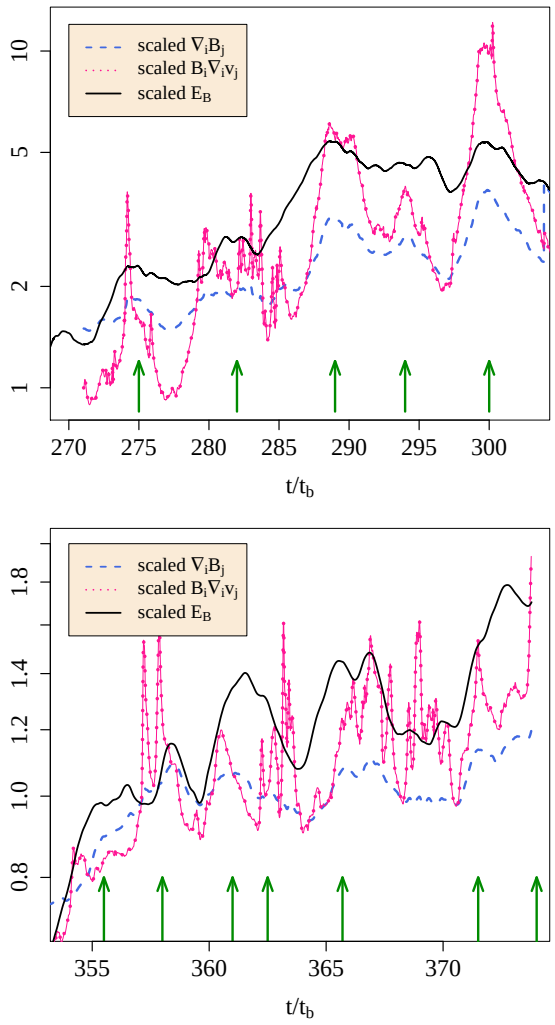

Fig. 1. Magnetic energy, E_B, is significantly amplified over long times due to repeated shear-bursts in (above) simulation g1 and (below) simulation g11 (parameters described in Table 1). The signature of the shear-burst, identified here with arrows, is clearly visible in the simultaneous peaks of the magnitude of the magnetic shear tensor $\nabla_i B_j$, and magnetic stretching tensor $B_i \nabla_i u_j$, which have been normalized to their initial-time values for easy comparison. The magnitude of the velocity shear tensor $\nabla_i v_j$ closely follows the magnetic shear. The magnitude of these tensors is calculated as a sum of the squares of the elements. Shear, and therefore magnetic stretching, drive the intermittent growth of magnetic energy.

The non-dimensional Boussinesq equations for MHD convection are:

$$\frac{\partial \boldsymbol{\omega}}{\partial t} - \nabla \times (\boldsymbol{v} \times \boldsymbol{\omega} + \boldsymbol{j} \times \boldsymbol{B}) = \hat{\nu} \nabla^2 \boldsymbol{\omega} - \nabla\theta \times \boldsymbol{g}_0 \quad (1)$$

$$\frac{\partial \boldsymbol{B}}{\partial t} - \nabla \times (\boldsymbol{v} \times \boldsymbol{B}) = \hat{\eta} \nabla^2 \boldsymbol{B} \quad (2)$$

$$\frac{\partial \theta}{\partial t} + (\boldsymbol{v} \cdot \nabla)\theta = \hat{\kappa} \nabla^2 \theta - (\boldsymbol{v} \cdot \nabla) T_0 \quad (3)$$

$$\nabla \cdot \boldsymbol{v} = \nabla \cdot \boldsymbol{B} = 0 \quad (4)$$

The equations include the solenoidal velocity field $\boldsymbol{v}$, vorticity $\boldsymbol{\omega} = \nabla \times \boldsymbol{v}$, magnetic field $\boldsymbol{B}$, current $\boldsymbol{j} = \nabla \times \boldsymbol{B}$. The quantity θ denotes the temperature fluctuation about a linear mean temperature profile $T_0(z)$ where z is the direction of gravity. The mean temperature, T_0, in equation 3 provides the convective drive of the system. The temperature fluctuation, θ, term in eq. 1 is the buoyancy force. The vector $\boldsymbol{g}_0$ is a unit vector in the direction of gravity. These equations are solved using a pseudospectral method with an adaptive-time-integration accomplished by a low-storage third-order Runge Kutta scheme (Williamson 1980).

Turbulent convective motion defines the characteristic time and length scales of the system: the large-scale buoyancy time, $t_b = (\alpha g |\nabla T_0|)^{-1/2}$ and temperature gradient length scale $L = T_*/\nabla T_0$ where T_* is defined by the root-mean-square of temperature fluctuations θ. α is the volume thermal expansion coefficient at constant pressure and g the gravitational acceleration (Gibert et al. 2006; Škandera & Müller 2009). The magnetic field is given in Alfvénic units, with Alfvén Mach number $v_0/v_A = 1$, $v_0 = L/t_b$. Three dimensionless parameters appear in the equations: $\hat{\nu}$, $\hat{\eta}$, and $\hat{\kappa}$. They derive from the kinematic viscosity ν, the magnetic diffusivity η, and thermal diffusivity κ and can formally be identified as the reciprocal value of classical Reynolds number, magnetic Reynolds number, and Péclet numbers, respectively (see Table 1 for definitions).

To investigate the influence of diffusivities on the shear-burst phenomena, parameters $\hat{\nu}$, $\hat{\eta}$, and $\hat{\kappa}$ are varied; consequently the simulations probe values of the Prandtl $\mathsf{Pr} = \hat{\nu}/\hat{\kappa}$ and the magnetic Prandtl number $\mathsf{Pr_m} = \hat{\nu}/\hat{\eta}$ spread between 0.5 and 2. The magnetic Prandtl number has been shown to exhibit a significant effect on small-scale dynamo action (Boldyrev & Cattaneo 2004; Schekochihin et al. 2005); the dependence of the dynamo mechanism on Prandtl number has been the subject of several wide-ranging investigations (Schmalzl et al. 2002; Maron et al. 2004; Simitev & Busse 2005). Realistically small Prandtl numbers cannot be reached with contemporary computer capabilities; in the solar convection zone generally expected values are $\mathsf{Pr_m} \sim 10^{-1} - 10^{-7}$ and in the earth's core $\mathsf{Pr_m} \sim 10^{-6}$. Simultaneously, Reynolds numbers are generally expected to be larger than can be computationally reached: $\mathsf{Re} \sim 10^{13}$ in the solar convection zone and $\mathsf{Re} \sim 10^{8}$ in the earth's core. Because of this discrepancy, the dynamical ranges of fluctuations in modern simulations are smaller than those expected in real systems. Our simulations thus present a first impression of the role of shear-bursts for astrophysical dynamos.

The numerical turbulence data in this work results from a set of simulations conducted with grid size 512^3, which constitutes high-resolution for the extremely long times treated here. These simulations are performed in a quasi-periodic slab or cube; the cube has a side of 2π, and the slab has slightly larger x- and y-directions of $(2\pi)^{3/2}$ to allow for the well-defined initial onset of the convective instability driving the turbulence (Chandrasekhar 1961). Our boundary conditions inhibit the formation of viscous boundary layers, which appear when impermeable boundary conditions are employed. The dissipative coefficients $\hat{\nu}$, $\hat{\eta}$, and $\hat{\kappa}$ parametrize the extent of the turbulent inertial range of scales, and in each simulation are chosen to be as small as possible so that the resolution constraint of $k_{max}\eta > 1.5$ is still satisfied (Pope 2000). Here, k_{max} is the largest resolvable wavenumber allowed by numerical resolution and η is the Kolmogorov length scale. The simulation parameters are summarized in Table 1. The Rayleigh number, characterizing the dynamical importance of buoyancy in Rayleigh-Bènard configurations, is of limited informative value for the present quasi-periodic system.

The initial state of the simulations contains fluctuations in a number of small k modes for the velocity, magnetic field, and temperature. The initial ratio of kinetic to magnetic energy of turbulent fluctuations is 10^6 with the kinetic energy of order unity. Fig. 2 shows a typical example of the initial time-evolution taken from simulation g2 of kinetic, E_v =

Table 1. Dimensionless simulation parameters: magnetic Reynolds number $\mathrm{Re_m}$, Péclet number Pe, Prandtl number $\mathrm{Pr} = \hat{\nu}/\hat{\kappa}$, magnetic Prandtl number $\mathrm{Pr_m} = \hat{\nu}/\hat{\eta}$, Rayleigh number Ra. The Reynolds number is defined as $\mathrm{Re} = (\mathrm{E_v} + \mathrm{E_B})^2/\nu(\epsilon_\mathrm{v} + \epsilon_\mathrm{B})$ where ϵ represents energy dissipation.

Simulation	g1	g2	g3	g4	g5	g6	g7	g8	g9	g10	g11
Re ($\times 10^3$)	3.3	6.1	5.7	5.8	2.1	5.8	5.0	2.4	1.5	4.0	3.6
$\mathrm{Re_m} = \mathrm{Pr_m Re}$ ($\times 10^3$)	6.6	6.1	5.7	2.9	3.6	8.7	10.	4.2	4.4	6.4	7.2
$\mathrm{Pe} = \mathrm{PrRe}$ ($\times 10^3$)	3.3	3.05	5.7	5.8	3.6	11.5	7.5	4.2	1.5	6.4	4.7
$\mathrm{Pr} = \hat{\nu}/\hat{\kappa}$	1	0.5	1	1	1.73	2	1.5	1.76	1	1.6	1.3
$\mathrm{Pr_m} = \hat{\nu}/\hat{\eta}$	2	1	1	0.5	1.73	1.5	2	1.76	3	1.6	2
$\mathrm{Ra} = (\hat{\nu}\hat{\kappa})^{-1}$ ($\times 10^5$)	2.5	2.2	2.5	4.4	1.44	2.2	1.67	0.9	0.3	3.8	1.7
$k_{\mathrm{max}}\eta$	2.0	1.6	1.8	1.74	2.1	2.5	2.35	3.22	4.1	1.7	2.0

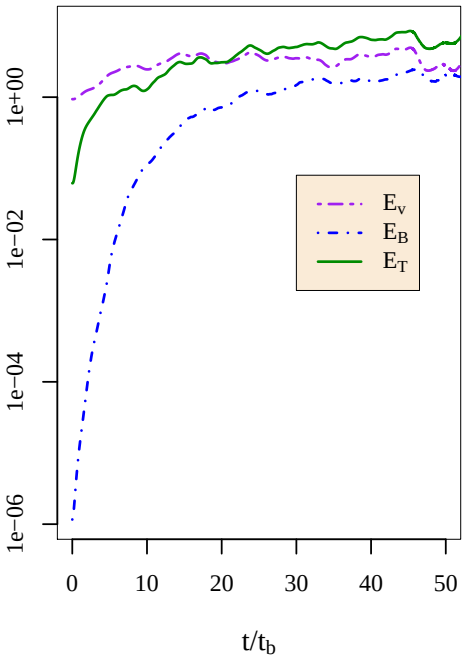

Fig. 2. Total kinetic, magnetic and thermal energies during the initial growth phase of the dynamo in simulation g2.

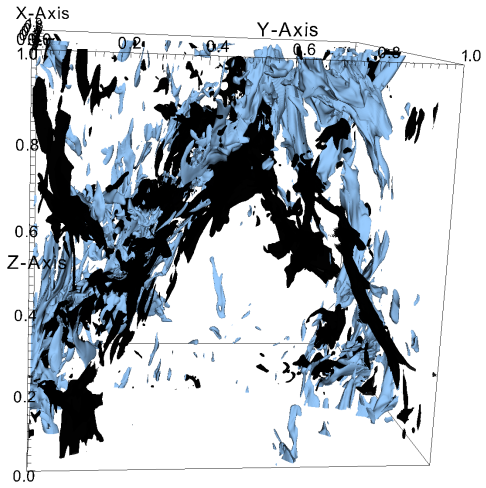

Fig. 3. A hot (black) flow moves upward vigorously, shearing against a cold (light blue) flow that moves downward. The shear along these opposing flows drives energy production during shear-bursts.

$V^{-1}\int_V \mathrm{d}V v^2/2$, magnetic, $E_B = V^{-1}\int_V \mathrm{d}V B^2$, and temperature, $E_T = V^{-1}\int_V \mathrm{d}V \theta^2$. The thermal energy should be understood as the variance of temperature fluctuations. Magnetic energy rises quickly due to small-scale dynamo action and saturates at $E_\mathrm{v}/E_B \approx O(1)$ characteristic of the quasi-stationary turbulent state of the MHD flow.

In Fig. 2 the steady-state global energies of the system evolve with fluctuations due to the convective motion. After a simulation reaches steady-state, energies fluctuate on the order of 10%, with a period of a 1-2 buoyancy times (see also Figure 5 of Cattaneo 1999a). During steady-state turbulent convection, we begin to observe a pattern of spontaneous longer periods (5-20 t_b) of significant growth in the global magnetic, thermal and kinetic energies. The energy variation during one such period can reach 10 times the steady-state energy level. For example, these periods of unusually elevated energy-growth occur 15 times over a time-span of 225 t_b in the simulation g1. The system can be regarded as statistically steady over periods of time significantly longer than the duration of a shear-burst.

A shear-burst centers around a period of increased growth magnetic energy that is accompanied by growth of both magnetic shear and magnetic stretching. Preceding the growth of magnetic energy, a coherent flow structure forms that has the appearance of high-velocity, thermally-polarized, coherent streams, in contrast to the typical situation with many smoothly convecting plumes of hot and cold fluid. These high-energy streams are strongly aligned in space, producing regions of high and increasing velocity and magnetic shear. The nonlinear shape and orientation of the high-energy streams differ for each shear-burst, displaying no preferred direction.

Shear causes magnetic field-line stretching, and thus amplification of magnetic energy (Childress & Gilbert 1995; Cattaneo 1999b). In Fig. 1 each shear-burst can be defined by a peak in magnetic shear that correlates with an increase in magnetic energy. Fig. 4 allows for closer inspection of the increase of magnetic, kinetic, and thermal energies for a typical isolated shear-burst in simulation g8; between $t = 225$ and $t = 235$ the energies increase by a factor of three. Individual shear-bursts can last from a couple buoyancy times to a couple tens of buoyancy times. At the peak of magnetic and kinetic energies, high energy hot and cold shearing becomes violent enough to break up the flow structures. The peak of global energy in Fig. 4 represents such an explosion of flow structures. The break-up of the fast streams spurs a slow decline in global energies. After the shear-burst has dissipated, the energies dissipate until the steady-state

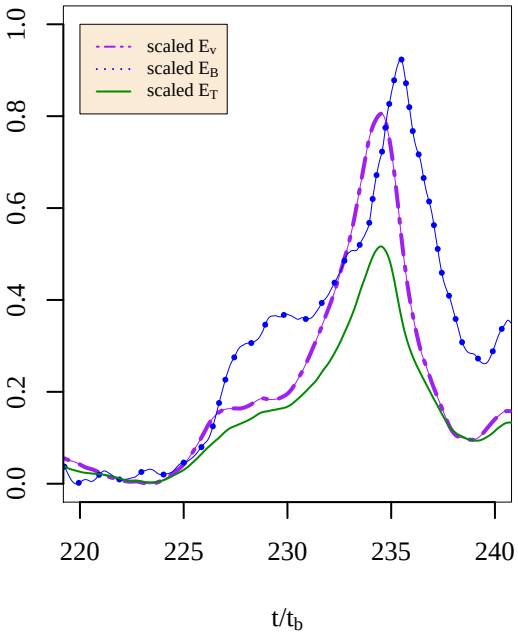

Fig. 4. The global kinetic energy E_v, magnetic energy E_B, and thermal energy E_T scaled to run between 0 and 1, for the span of a typical shear-burst in simulation g8.

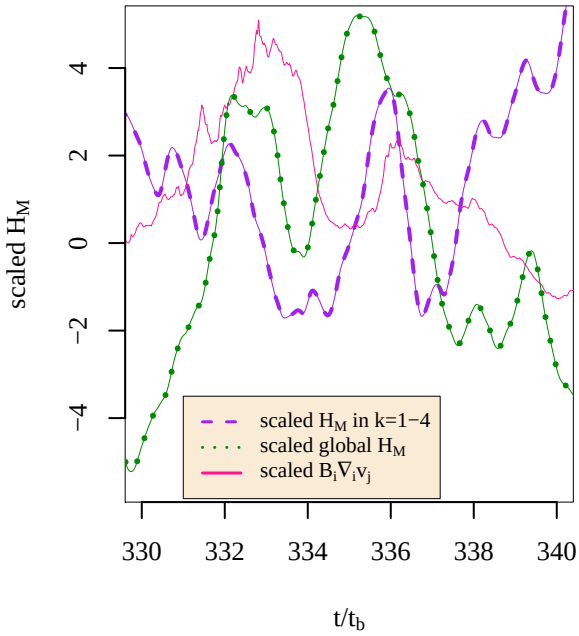

Fig. 5. The characteristic double-peak from two closely spaced shear-bursts in simulation g11 is visible in magnetic helicity. The magnetic helicity H_M at low-wavenumbers k is shown scaled to its initial time-value with sign preserved. Magnetic helicity quantities are shown scaled to their initial time values in a way that preserves sign. The magnitude of the magnetic stretching tensor is shown shifted and scaled to fit the scale of the magnetic helicity, to provide a time-reference for the shear-bursts.

level maintained by the fluctuation dynamo has been reached. Shear-bursts can overlap in time, and also can occur closely in sequence, as shown in Fig. 1.

The lifetime and magnitude of the energy growth, in particular the peak in thermal energy, can vary greatly between simulations and even between shear-bursts in the same simulation. This shows no apparent dependence on the Prandtl numbers. That the Prandtl numbers do not directly impact the shear-burst phenomena is surprising because the Prandtl numbers express the ratio of turbulent intensities and dynamic ranges of the respective turbulent fields. This relationship between Prandtl numbers and the turbulence can be understood by relating the Prandtl numbers to the ratios of Reynolds numbers, $\mathsf{Pr} = \mathsf{Pe}/\mathsf{Re}$ and $\mathsf{Pr_m} = \mathsf{Re_m}/\mathsf{Re}$, where the Péclet number can be regarded as the same structure as a Reynolds number for thermal fluctuations.

The characteristic length-scale of Boussinesq convection is the Bolgiano-Obukhov length, $\ell_{\rm bo} = \epsilon_v^{5/4}/\epsilon_T^{3/4}$ that separates convectively-driven scales of the flow $\ell > \ell_{\rm bo}$ from the range of scales where the temperature fluctuations behave as a passive scalar $\ell < \ell_{\rm bo}$. In this definition ϵ_v and ϵ_T are the kinetic and thermal energy dissipations respectively. Typically in our convection simulations $\ell_{\rm bo}$ is comparable to the system size so only the largest scales in the flow are convectively driven. The shear-bursts are large scale phenomena by this classification, but not dominated by convective motion. This suggests an explanation for the apparent insensitivity to changes in the Prandtl numbers.

Although insensitive to the Prandtl numbers, the shear-bursts interact nonlinearly with the turbulent environment, mainly via large-scale magnetic structure. This is reflected in the behavior of magnetic helicity, $H_M = V^{-1}\int_V \mathrm{d}V\boldsymbol{A}\cdot\boldsymbol{B}$, which measures the linkage and knottedness of the magnetic field-lines (Biskamp 2000; Moffatt 1978). A signature of the shear-burst is the growth of global magnetic helicity as the shear flows strengthen. Magnetic helicity is not conserved in the dissipative system we study, and this growth of magnetic helicity typically exceeds more than a standard deviation from the average magnetic helicity over the time-span of the simulation. A peak of global magnetic helicity frequently shortly precedes or coincides with a shear-burst. Fig. 5 shows the typical time-evolution of the magnetic stretching against the growth of global magnetic helicity and magnetic helicity at the largest scales. In the time pictured, two shear-busts occur within 5 t_b, and a clear double-peak structure is also visible in the magnetic helicity.

The magnetic helicity grows particularly in low wavenumbers k, associated with the growth of an isolated structure with a strong helicity polarity; this low-k growth is a signature of an ongoing inverse spectral transfer of magnetic helicity common for 3D MHD systems (Müller et al. 2012; Biskamp 2003; Alexakis et al. 2008). The dramatic change in the bias of magnetic helicity in the system during one shear-burst is shown in Fig. 6; in Fig. 5 the large-scale magnetic helicity of the structures spawned has negative polarity in the two shear-bursts pictured. Large-scale magnetic helicity structures persist longer than the high-energy shear streams, and longer than it takes for the global energies to taper off. Because the magnetic helicity experiences an inverse cascade and our system has small dissipation this is theoretically expected.

Shear-bursts change the magnetic helicity because they generate significant currents through magnetic shear. When no shear-burst is present in the system small filaments of high-current are common and likely indicate slow reconnection on small scales. However when a shear-burst grows, large-scale high-current structures grow at the same time. A typical growth in current around a shear-burst is shown in Fig. 7.

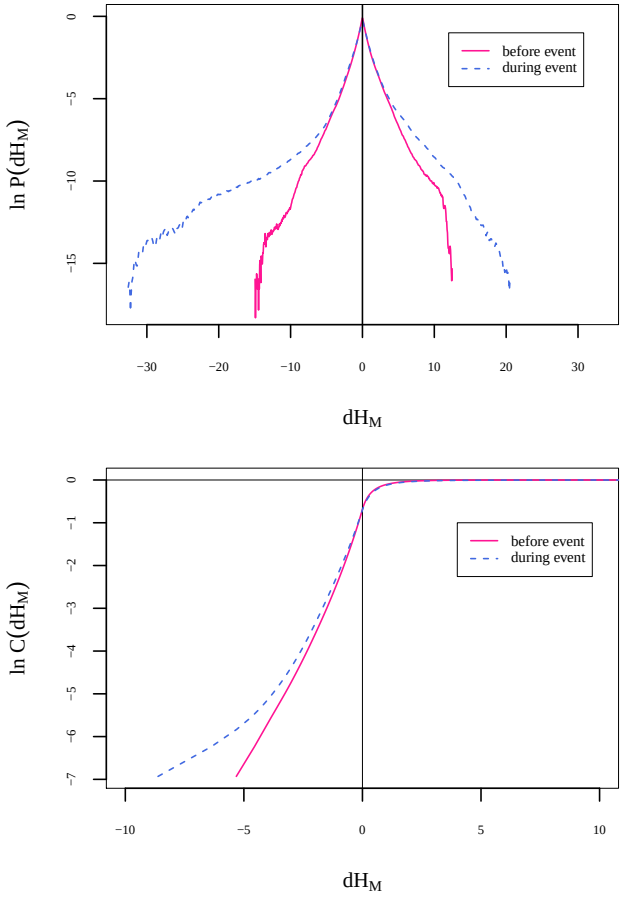

Fig. 6. (Above) probability distribution and (below) cumulative distribution of local magnetic helicity, *i.e.* $dH_M = \boldsymbol{A} \cdot \boldsymbol{B}$ in the simulation volume before and during a shear-burst in simulation g1. During this shear-burst, as the global magnetic helicity grows, the tail of negative magnetic helicity grows, and grows much higher than the positive tail.

1. Conclusions

We have isolated a characteristic mechanism of dynamo action in MHD convection that operates through spontaneously-developing intermittent bursts of high shear. Because this process is robust and general, it is of potential importance for astrophysical small-scale dynamo action in turbulent convection scenarios. These shear-bursts consist of the formation of large, coherent, highly-sheared flows along-side magnetic structures with a magnetic-helicity polarity bias. The increasing shear causes a gradual rise of energy at all spatial scales due to magnetic stretching in the system over several buoyancy times. After some time, the shear flows become so highly aligned that their violent shearing breaks up the flow structure. Once the shear flows are destroyed, the elevated energy dissipates over several buoyancy times. Closely-spaced shear-bursts often occur in a series, creating long periods of time where magnetic energy is elevated significantly above the steady-state.

Acknowledgements. This work has been supported by the Max-Planck Society in the framework of the Inter-institutional Research Initiative Turbulent transport and ion heating, reconnection and electron acceleration in solar and fusion plasmas of the MPI for Solar System Research, Katlenburg-Lindau, and the Institute for Plasma Physics, Garching (project MIFIF- A-AERO8047).

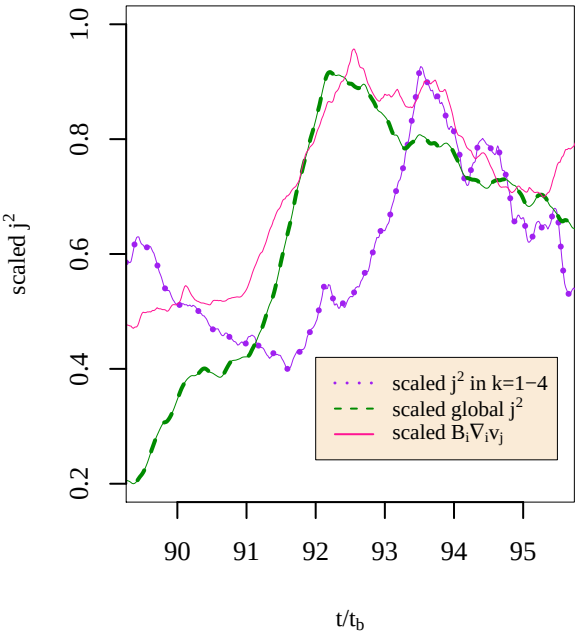

Fig. 7. Current-squared in the lowest wavenumbers $k = 1, 2, 3, 4$ scaled to its initial time-value during a shear-burst in simulation g2. Global current-squared and magnetic shear are shown scaled and shifted to fit on the same scale for reference.

References

Alexakis, A., Mininni, P. D., & Pouquet, A. 2008, The Astrophysical Journal, 640, 335
Biskamp, D. 2000, Magnetic Reconnection in Plasmas (Cambridge: Cambridge University Press)
Biskamp, D. 2003, Magnetohydrodynamic Turbulence (Cambridge: Cambridge University Press)
Böhm-Vitense, E. 2008, The Astrophysical Journal, 657, 486
Boldyrev, S. & Cattaneo, F. 2004, Physical Review Letters, 92, 144501
Calzavarini, E., Doering, C. R., Gibbon, J. D., et al. 2006, Physical Review E, 73, 035301(R)
Cattaneo, F. 1999a, in Motions in the solar atmosphere: proceedings of the summerschool and workshop held at the Solar Observatory Kanzelhöhe Kärnten, Austria, September 1-12, 1997, ed. M. M. Arnold Hanslmeier (Springer Verlag)
Cattaneo, F. 1999b, The Astrophysical Journal Letters, 515, L39
Cattaneo, F., Emonet, T., & Weiss, N. 2003, The Astrophysical Journal, 588, 1183
Chandrasekhar, S. 1961, Hydrodynamic and hydromagnetic stability (Oxford: Oxford University Press)
Childress, S. & Gilbert, A. D. 1995, Lecture Notes in Physics Monographs: Stretch, twist, fold: the fast dynamo, Vol. 37 (Springer Verlag)
Christensen, U. R., Holzwarth, V., & Reiners, A. 2009, Nature, 457, 167
Cline, K. S., Brummell, N. H., & Cattaneo, F. 2003, Astrophys. J., 599, jILA Pub. 7195
Gibert, M., Pabiou, H., Chillà, F., & Castaing, B. 2006, Physical Review Letters, 96, 084501
Güdel, M., Guinan, E. F., & Skinner, S. L. 1997, The Astrophysical Journal, 483, 947
Harder, H. & Hansen, U. 2005, Geophysical Journal International, 161, 522
Maron, J., Cowley, S., & McWilliams, J. 2004, The Astrophysical Journal, 603, 569
McFadden, P. & Merrill, R. 1995, Physics of the Earth and Planetary Interiors, 91, 253
Moffatt, H. 1978, Magnetic Field Generation in Electrically Conducting Fluids (Cambridge University Press)
Moll, R., Graham, J. P., Pratt, J., et al. 2011, The Astrophysical Journal, 736, 36
Müller, W.-C., Malapaka, S. K., & Busse, A. 2012, Physical Review E, 85, 015302
Olson, P. L., Glatzmaier, G. A., & Coe, R. S. 2011, Earth and Planetary Science Letters, 304, 168
Pope, S. B. 2000, Turbulent Flows (Cambridge: Cambridge University Press)
Reiners, A. & Basri, G. 2007, The Astrophysical Journal, 656, 1121

Schekochihin, A. A., Haugen, N. E. L., Brandenburg, A., et al. 2005, The Astrophysical Journal, 625, L115
Schmalzl, J., Breuer, M., & Hansen, U. 2002, Geophysical & Astrophysical Fluid Dynamics, 96, 381
Simitev, R. & Busse, F. 2005, Journal of Fluid Mechanics, 532, 365
Simon, T., Ayres, T. R., Redfield, S., & Linsky, J. L. 2008, The Astrophysical Journal, 579, 800
Stanley, S. & Glatzmaier, G. A. 2010, Space science reviews, 152, 617
Stevenson, D. J. 2010, Space science reviews, 152, 651
Tobias, S. M., Cattaneo, F., & Brummell, N. H. 2011, The Astrophysical Journal, 728, 153
Škandera, D. & Müller, W.-C. 2009, Physical Review Letters, 102, 224501
Weiss, N. & Thompson, M. 2009, Space Science Reviews, 144, 53
Wilkin, S. L., Barenghi, C. F., & Shukurov, A. 2007, Physical review letters, 99, 134501
Williamson, J. H. 1980, Journal of Computational Physics, 35, 48
Zeldovich, Y. B., Ruzmaikin, A. A., & Sokoloff, D. D. 1983, Magnetic Fields In Astrophysics (New York: Gordon and Breach Science Publishers)